23rd ABCM International Congress of Mechanical Engineering
December 6-11, 2015, Rio de Janeiro, RJ, Brazil

MicroPIV and Numerical Characterization of Microfluidic Flow: Quantitative Velocity Profiles, Channel Geometries, and Flow Rates

M. J. B. Moura
Dept. Mech. Eng., PUC-Rio, R. Marquês de São Vicente, 225, Gávea, Rio de Janeiro, Brazil
mariamoura@puc-rio.br

P. W. Bryant
IBM Research – Brazil, Av. Pasteur 138, Urca, Rio de Janeiro, CEP 22290-240, Brazil
pbryant@br.ibm.com

R. F. Neumann
IBM Research – Brazil, Av. Pasteur 138, Urca, Rio de Janeiro, CEP 22290-240, Brazil
rneumann@br.ibm.com

M. Steiner
IBM Research – Brazil, Av. Pasteur 138, Urca, Rio de Janeiro, CEP 22290-240, Brazil
msteine@us.ibm.com

M. S. Carvalho
Dept. Mech. Eng., PUC-Rio, R. Marquês de São Vicente, 225, Gávea, Rio de Janeiro, Brazil
msc@puc-rio.br

C. Feger
IBM Research – Brazil, Av. Pasteur 138, Urca, Rio de Janeiro, CEP 22290-240, Brazil
feger@us.ibm.com

Abstract. *Microscopic Particle Image Velocimetry (μPIV) is a technique used to obtain velocity fields of fluid flow at the microscale. In practice, this technique is complicated by the fact that one must sample optically over a finite volume, over which significant variations of the velocity fields can occur. For this reason μPIV measurements have only been used to obtain qualitative results, unless the finite volume effects were corrected through the use of convoluted data processing methods. Here we present a new method that combines the analysis of experimental data and numerical simulations for obtaining quantitative velocity profile information. Our method allows one to obtain the size and shape of the effective volume over which moving fluids are sampled. We also show how the method permits one to infer either the channel geometry, the flow rate, or the velocity field for a system where one of these quantities is not known. This method not only provides quantitative results, but also increases the simplicity and utility of μPIV measurements.*
Keywords: *Microfluidics, Particle Image Velocimetry, Sampling Volume*

1. INTRODUCTION

Micro Particle Image Velocimetry (μPIV) is the state of the art for measuring fluid flow profiles in channels that have dimensions in the microscale (Lindken *et al.*, 2009). Based on the motion of microscopic tracer particles flowing with the fluids, one can infer a projection of the velocity field of the fluid (Meinhart *et al.*, 1999). The technique is indispensable for research and development in any field in which the motion of fluids through microchannels is important (Williams *et al.*, 2010; Cierpka and Kähler, 2012), such as biology, nanotechnology, petroleum, and manufacturing.

Experimenting on small systems is inherently difficult, and one particular difficulty for μPIV results from the existence of a finite domain over which one images the tracer particles. When this domain is small compared to length scales over which velocity gradients change appreciably, one can simply ignore the volume of this finite domain, as demonstrated by Joseph and Tabeling (2005) and Tsai *et al.* (2009). However, when the features to be observed approach the size of the system itself, one must use μPIV with a large depth of field. As a consequence, velocity fields often change significantly over the domain that is sampled. The interpretation of measurement results in this case is complicated (Kloosterman *et al.*, 2011; Olsen and Adrian, 2000; Rossi *et al.*, 2012).

As a consequence, in the past one has often been limited to evaluating μPIV results qualitatively, for example considering only profile shapes in the centers of channels, and has ignored the magnitude of the velocity field (Meinhart *et al.*, 1999; Sott *et al.*, 2013). To achieve more quantitative results, one has treated the effects of the finite domain as errors, and has attempted to correct these errors using post-processing techniques (Kloosterman *et al.*, 2011; Rossi *et al.*, 2012; Westerweel *et al.*, 2004; Cierpka and Kähler, 2012). In an effort to simplify μPIV and to measure quantitatively the velocity fields in microchannels, we introduced the concept of the Sampling Volume (SV), which is defined as the region over which one must average the velocity field to recover the measured velocity profiles (Bryant *et al.*, 2014). We also showed that, to within experimental uncertainties, a simple, rectangular SV suffices to explain measurements for a wide range of μPIV experiments.

Considering the SV, many of the typically ignored or discarded features in measured profiles can in fact be kept and used to infer the entire velocity field in a microchannel, quantitatively, from wall to wall. Alternatively, these features can be used to infer the cross-sectional shape of microchannels with unknown geometry. Here we explain the concept of the SV and this process of inferring an unknown geometry, whereby one iterates over unknown channel cross sections to identify which channels are consistent with measurements and which are not.

We begin in Section 2. with a general description of μPIV, and we introduce the theory of the SV. In Section 3. we present a sample of the experimental verification of this theory. Section 4.details how velocity fields or channel geometry can be inferred from a simple μPIV measurement.

2. μPIV WITH LARGE DEPTH OF FIELD

2.1 Basic principles of μPIV

In Microscopic Particle Image Velocimetry (μPIV), one observes the motion of fluorescent tracer particles seeded in flowing fluids, and based on the motion of these particles calculates two-dimensional projections of the velocity field of the fluid. In principle, the technique is quite simple. One images the particles' locations at two times separated by a duration Δt and then from the images calculates the displacements, $\Delta \mathbf{d}$, of the particles. The average velocity of the particles during the interval between images is then $\mathbf{v} = \Delta \mathbf{d}/\Delta t$. Assuming the tracer particles faithfully follow the motion of the fluid, $\mathbf{v}$ is the average velocity of the fluid itself.

A laser providing light at the excitation frequency of the fluorescent tracer particles illuminates them as they move through the microchannel. The particles subsequently fluoresce, and emitted light passes through a filter that blocks the excitation light. The emitted light thus provides an image of the tracer particles, and a microscope magnifies the image before it is recorded on a CCD camera.

μPIV is complicated by the presence of many particles in each image. Furthermore, for flow in microchannels, the particles must be small enough that many can pass simultaneously through the channel without significantly disturbing the flow. As a consequence, the particles are susceptible to Brownian motion. Instead of tracking individual particles, then, one uses correlation techniques to determine the net displacements of ensembles of particles found within two-dimensional "interrogation windows" of finite size. Figure 1(a) is a schematic of the view of the channel and the particles, as seen from the camera. The grid drawn in dashed lines represents the interrogation windows. Their sizes are exaggerated for clarity. The result of this processing is a two-dimensional projection of the three-dimensional velocity field covering all of the fluid in which particles appear in the images with intensity sufficient to affect the particle identification and subsequent correlation algorithms.

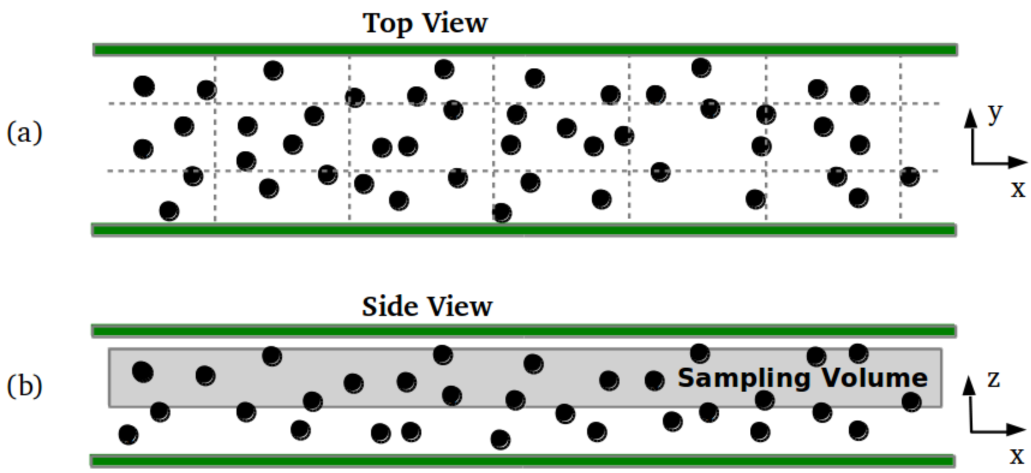

Figure 1. (a) Schematic of μPIV, showing particles viewed from the camera. The grid drawn in dashed lines represents the interrogation windows. (b) Schematic of the side view.

In Fig. 1(b) is a schematic side view of a μPIV channel. The shaded rectangle represents the finite region over which particles are resolved and contribute to the measured velocity. Ideally, one would expect this region to be centered with respect to the channel, but this need not be the case, in general. Below, we will call this region the Sampling Volume (SV), and we will show that, to within experimental uncertainties, a simple rectangular solid suffices to explain our measured velocity profiles.

The depth of the SV depends on the optical setup as well as on the algorithms that interpret camera images and calculate correlations and displacements. In the past, it has been assumed that the accuracy of the measured velocity field is limited by the presence of this finite region. To improve accuracy, then, one has treated its effects as errors and has tried to remove these errors by means of complicated post-processing (Kloosterman *et al.*, 2011; Rossi *et al.*, 2012; Westerweel *et al.*, 2004; Cierpka and Kähler, 2012).

2.2 Average over the Sampling Volume

As an alternative to the use of post-processing to eliminate the effects of a finite sampling domain, Bryant *et al.* (2014) introduced a method in which the finiteness is taken into account, and by which a μPIV experiment can be calibrated. The SV is defined as the volume over which one averages the three dimensional velocity field, $\mathbf{v}(x, y, z)$, of the flowing fluid to reproduce measured profiles. For simplicity we will consider here only velocity profiles in channels with a constant cross section in the x, or streamwise, direction. By symmetry, $\mathbf{v}(x, y, z) \to \mathbf{v}(y, z)$, and the velocity field averaged over the SV is

$$\langle \mathbf{v} \rangle_{SV}(y) = \frac{\int_{z_-(y)}^{z_+(y)} dz\, \mathbf{v}(y,z)}{z_+(y) - z_-(y)}, \tag{1}$$

as a function of y, which is the direction across the channel. Here the integration bounds are defined for a rectangular SV by

$$z_- \equiv \text{Max}\left(c - \frac{\delta}{2}, z_{\text{bot}}(y)\right) \tag{2}$$

and

$$z_+ \equiv \text{Min}\left(c + \frac{\delta}{2}, z_{\text{top}}(y)\right). \tag{3}$$

In Equations (2) and (3), $\text{Max}(\cdot)$ and $\text{Min}(\cdot)$ denote the maximum and minimum values of the arguments. We use $z_{\text{bot}}(y)$ and $z_{\text{top}}(y)$ to denote the bottom and top locations of the channel, respectively, as functions of y. For simple channels, these functions uniquely define the channel cross section. The vertical center of the SV is c, where we choose $c = 0$ for a SV centered in the channel. The thickness of the SV is represented by δ.

$\langle \mathbf{v} \rangle_{SV}(y)$ from Equation (1) is to be compared with velocity profiles measured in μPIV experiments. To make a quantitative comparison, one must know the expected velocity field, $\mathbf{v}(y, z)$, of the flowing fluid. For non-trivial channel geometry, $\mathbf{v}(y, z)$ must be numerically simulated to a precision high enough that one can judge $\langle \mathbf{v} \rangle_{SV}(y)$ to within experimental uncertainty. We used the Lattice Boltzmann method (LBM) (Chen and Doolen, 1998) to simulate $\mathbf{v}(y, z)$ for various channel cross sections, as described below.

3. EXPERIMENT

3.1 Experimental setup

For all experiments in this paper we used a glass microfluidic device (Dolomite Center Ltd) with a straight channel of elliptical cross-section, with semi-minor axis of (50 ± 1.5) μm and semi-major axis of (55 ± 1.5) μm. We determined the uncertainty in the axes by digitizing images from a Scanning Electron Microscope. We mixed purified water (Thermo Scientific Nalgene Analytical Filter, 0.2 μm) with a solution of fluorescent particles (ex/em 542/612 nm, Thermo Scientific Fluoro-Max Dyed Red Aqueous Fluorescent Particles, 1 μm in diameter). The optimum mix for these experiments was 86% water to 14% fluorescent particle solution at 1.81×10^{10} beads/ml, and it was chosen so that there were approximately 10 fluorescent particles within each interrogation window, in order to provide a reasonable signal-to-noise ratio in the determination if the average displacement using the cross-correlation of snapshots.

We injected the fluid mix using a syringe pump (11 Elite syringe pump 704501, Harvard Apparatus). According to the manufacturer, the syringe pump has an uncertainty in the flow rate of 0.5%. Injection rates ranged from 75 μl/h to 100 μl/h.

The measured velocity fields were obtained using a commercially available μPIV system (TSI Inc.). The system is composed of a microscope, two lasers, a CCD camera, and a laser pulse synchronizer. The inverted microscope (Olympus X71S1F-3) has a 10X/0.3 air objective (UPlanFL N, Olympus). The CCD camera (Sensicam 630166, PowerView, 1.4MP) has resolution of 1376 $\times$ 1024 pixels and a 2X projection lens. For this experimental setup the camera's field of view is

(440±5) μm × (325±5) μm. One pixel therefore corresponds to 0.32 μm in both x and y directions. The two Nd:YAG pulsed lasers (Gemini PIV-15, NEW WAVE RESEARCH) operate at wavelength of 532 nm, a frequency of 15 Hz, and a pulse energy of 50 mJ. A laser pulse synchronizer (610034, TSI Inc.) controls the time interval between the laser pulses, Δt, and time of exposure of the CCD. The system is operated by the software Insight 3G (TSI Inc.), that performs data acquisition as well as image processing. For each experiment 100 pairs of images were collected with a Δt of 500 μs. For the chosen processing methods, the overall resolution is 5.12 μm. For a detailed description of the image processing methods, see Bryant *et al.* (2014).

3.2 Experimental Results and Verification

We have verified that, to within experimental uncertainty, averaging over a rectangular SV explains our results for a wide variety of experiments in straight channels. Our results indicate that the change in refraction index between the surrounding air and the liquid media inside the channel was not significant relative to other uncertainty or, at least, not significant enough to require a non-trivial SV shape. In Fig. 2 is a comparison for a volumetric flow rate of 75 μl/h.

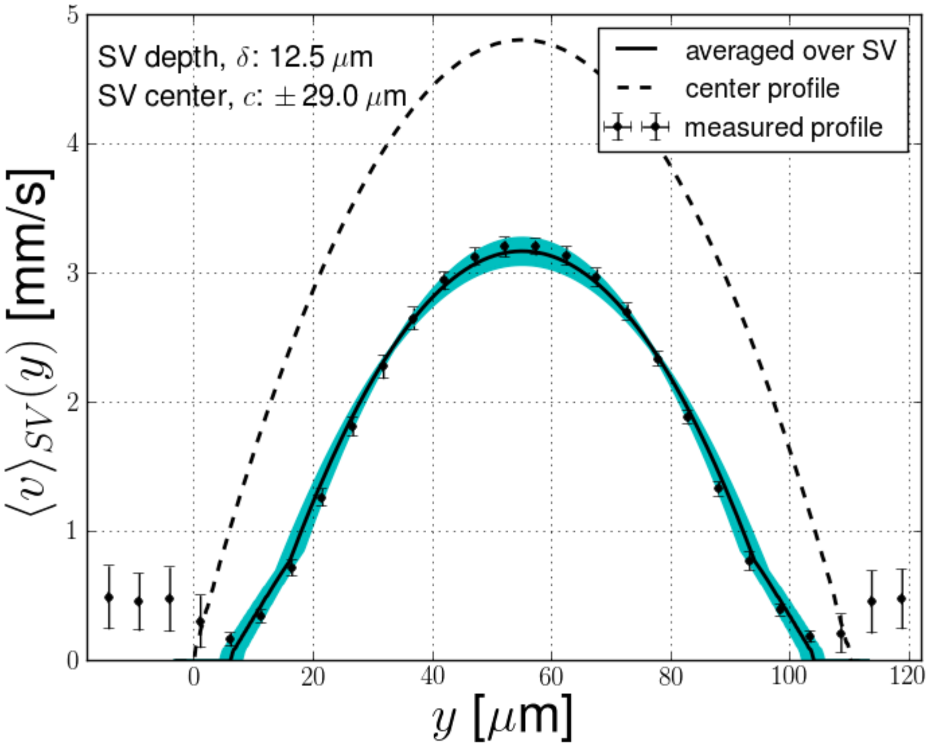

Figure 2. Comparison of $\langle v\rangle_{SV}(y)$, calculated with Equation (1), and the measured profile

The solid line is $\langle v\rangle_{SV}(y)$, and the shaded area represents the combined uncertainty in the channel cross section and the volumetric flow rate, as discussed in Section 3.1and in Bryant *et al.* (2014). The dots represent the measured speed at y, averaged over 85 profiles spread along the streamwise direction. The vertical error bars represent one standard deviation. Horizontal error bars from length calibration of the microscope are too small to be seen. The dashed line would be the measured profile for a centered SV of zero thickness. The non-zero speeds beyond the channel walls are numerical artifacts from correlation algorithms used to identify the displacements of particles.

To fit the data in Fig. 2, we used as free parameters only the position of the SV center, c, and its thickness, δ. The result indicates that $\delta = 12.5$ μm and $c = \pm 29.0$ μm. Because of the symmetry of the microchannel with respect to its axis, the position of the SV center can be positive or negative. In Fig. 3 is a schematic showing the SV overlaid on a simulation of the speed field of the fluid. The dashed line through the channel center corresponds to the center profile shown by a dashed line also in Fig. 2. In this experiment, the vertical (z) variation of the velocity field within the SV reaches up to 20% of the maximum velocity.

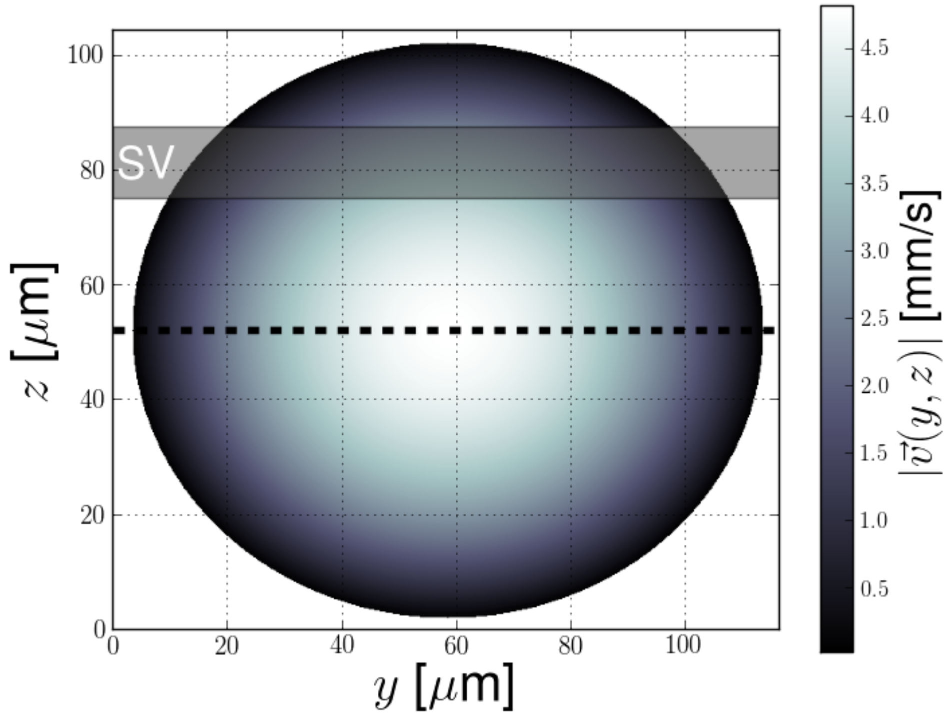

Figure 3. Simulated speed field of the fluid overlaid by the SV that results in the fit in Fig. 2. The dashed line is at the center of the channel.

4. MEASURING MICROSCOPIC VELOCITY FIELDS

4.1 Using the entire profile

By acknowledging the presence of the SV and minimizing the amount of post-processing required, features in the measured velocity profiles, such as the two kinks near the walls in the profile in Fig. 2, can be interpreted physically in a straightforward manner. By comparing the velocity profile with Fig. 3, one can see that the span in y of the profile together with the position of the kinks uniquely determine the position and size of the rectangular SV. The endpoints of the measured profile, where the speed goes to zero, correspond to the intersection of the bottom of the SV in Fig. 3 with the channel walls. The kinks in the theoretically calculated profile occur when the integration bound z_{+} in Equation (3) switches from $c + \delta/2$ to $z_{\text{top}}(y)$. This means the position of the kinks define the intersection of the top of the SV with the channel walls.

In this experiment, the only other possible position of the SV can be found by reflecting Fig. 3 through the plane bisecting it horizontally. The measured profile would be the same for the reflected system, so as far as the measurement is concerned, the SV can be uniquely defined from this single experiment. Note that this is not always the case. In general, based only on the span of a profile and the location of its features, there may be multiple possibilities for the disposition of the SV. The uniqueness of the SV and the ease with which it can be determined depend on the channel geometry, the experimental uncertainties, and the SV itself.

With the disposition of the SV determined, one can use Equation (1) to find the velocity field, $\mathbf{v}(y, z)$, that results in a match with the measured profile. For a wide variety of microfluidics systems, in which fluids are often Newtonian and flow is often laminar, $\mathbf{v}(y, z)$ can be completely determined by only a few parameters such as flow rate, fluid properties, and perhaps surface wettability. A fit to the measured profile, then, offers a way to infer these parameters from a μPIV measurement.

For example, we know the cross section of the microchannel used in the experiment pictured in Fig. 2. Had we not known the flow rate delivered by the pump, based on the velocity profile we could have determined it to be 75 μl/h by performing several flow simulations with varying flow rates until a fit to the experimental data was obtained, determining the correct flow rate up to experimental uncertainty. We could have therefore inferred the velocity field of the fluid throughout the entire microchannel, including in the domain not covered by the SV. This type of quantitative determination of flow characteristics using μPIV with a large depth of field promises to increase the utility of the measurement technique greatly.

4.2 Inferring channel cross sections

Interestingly, one can also use μPIV with the SV to determine the cross section of a microchannel of unknown geometry. For the same reasons described in the previous section, the determination may or may not be unique, and must always be made with care. Even if it is not unique, however, one can eliminate a shape as a possible cross section, or assess the likelihood of various shapes within the set of possible cross sections.

Figure 4 is an example of the result of fitting a measured profile to the SV calculated for the elliptical cross section measured by the SEM and described above. For this experiment, the pump delivered a flow rate of 100 μl/h. As before,

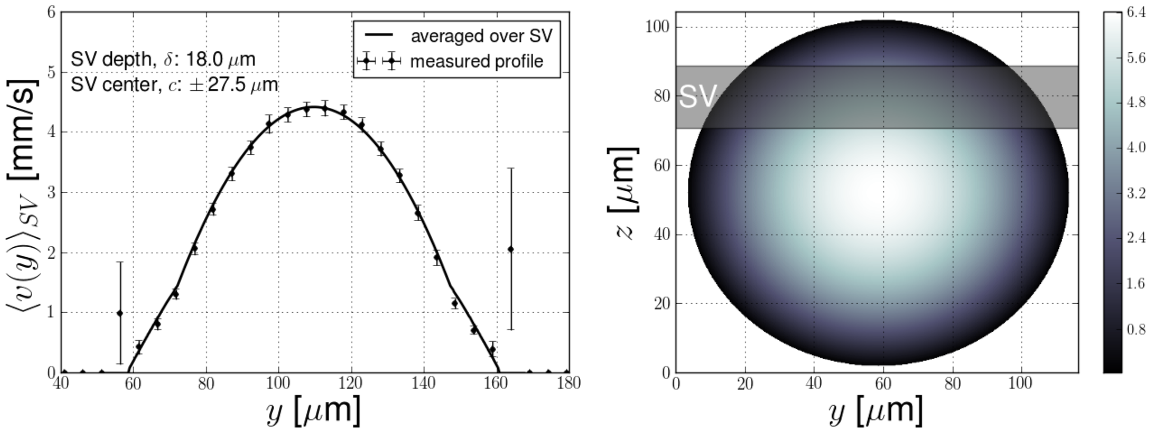

Figure 4. Fit to the measured speed profile for the elliptical cross section, and an overlay of the resulting SV on the simulated velocity field

when averaging over the velocity field, $\mathbf{v}(y, z)$, simulated for the known, elliptical channel cross section, the fit is good.

In Fig. 5 is an attempt to fit the same measured profile using $\mathbf{v}(y, z)$ for a cylindrical cross section of diameter 107 μm and the same fluid flow rate. The SV was positioned to result in the correct profile span and the correct positions of the

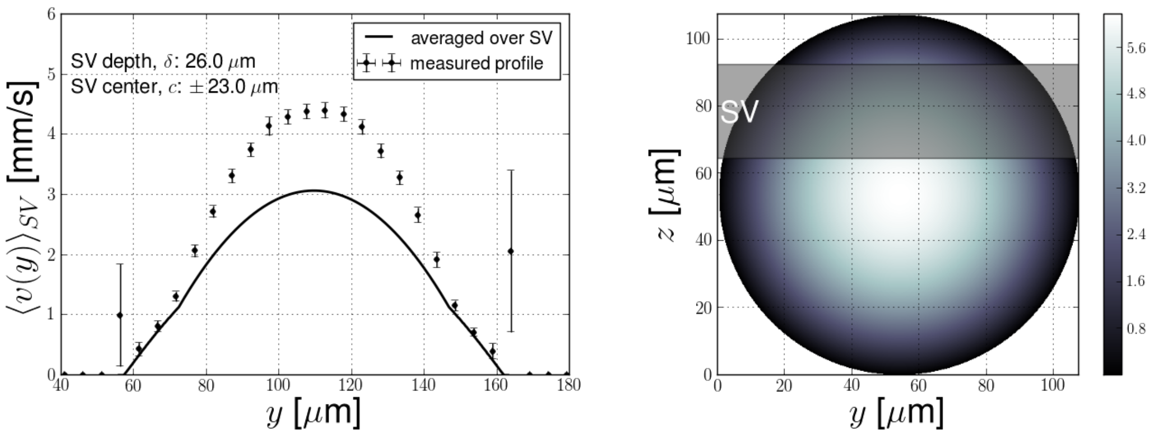

Figure 5. Fit to the measured speed profile for a cylindrical cross section, and an overlay of the resulting SV on the simulated velocity field

kinks. This results in a bad fit in the center of the profile. Similarly, an SV that results in a good fit in the center gives a bad fit near the walls. The measured profile will not result from flow in a cylindrical cross section.

We have also compared the calculated and measured profiles for more complicated rectangular cross sections with rounded corners. These cross sections are modeled as the intersection of a rectangle of width 110 μm and height 100 μm, with a circle and an ellipse. Figure 6 shows the result for the intersection of the rectangle with a circle of radius 56 μm. To match the profile span and the positions of the kinks, the SV must be positioned as shown on the right hand side. While the predicted profile is closer to the measured profile, it is still not a good fit. This cross sectional shape can also be eliminated as a candidate. Figure 7 shows the result for the intersection of the rectangle with an ellipse of semi-major and semi-minor axes of 58 μm and 51 μm, respectively. In this case, the fit is as good as the fit for the known geometry shown in Fig. 4.

Based only on a comparison between Fig. 4 and 7, one may not be able to decide which of the two cross sections is more likely. One can, however, use additional information to make an informed judgment. For example, Bryant

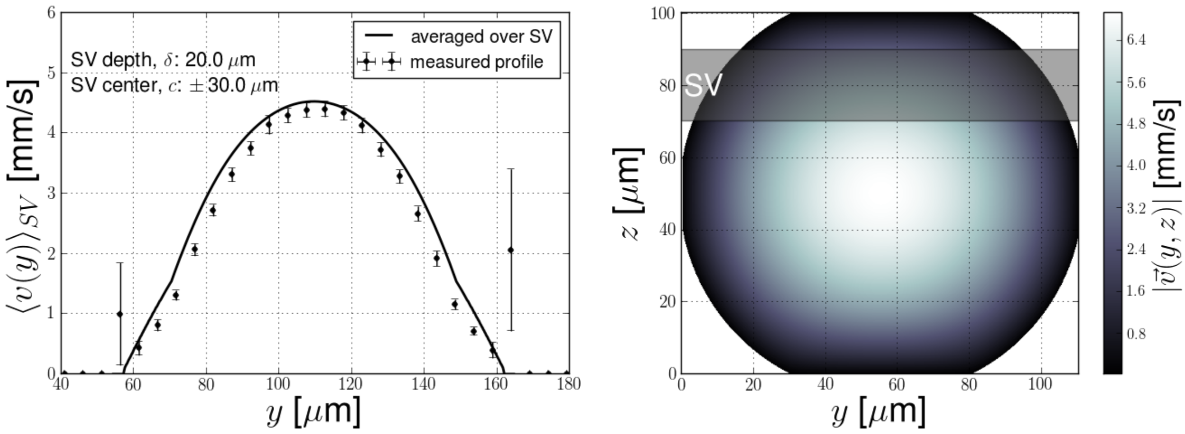

Figure 6. Fit to the measured speed profile and the resulting SV for a cross section modeled as the intersection of a 110 μm by 100 μm rectangle with a circle of radius 56 μm

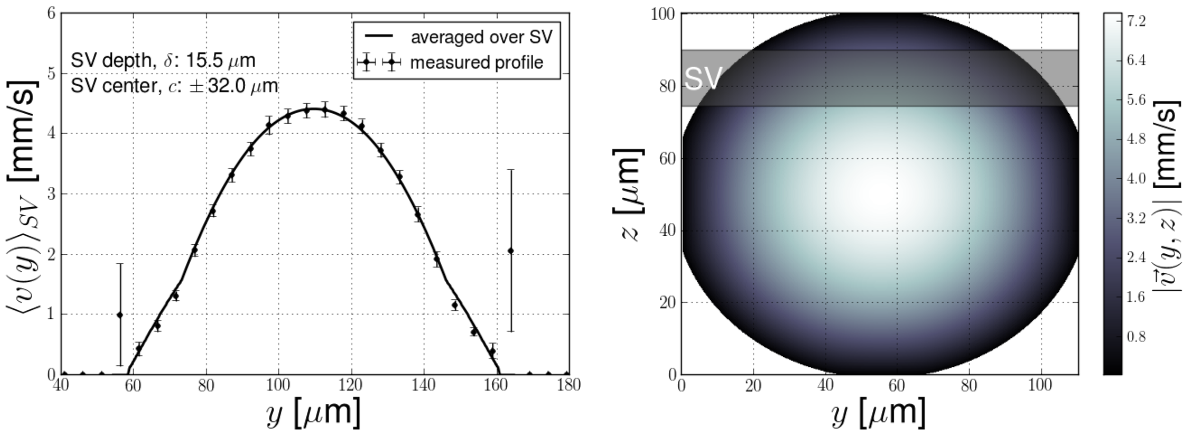

Figure 7. Fit to the measured speed profile and the resulting SV for a cross section modeled as the intersection of a 110 μm by 100 μm rectangle with an ellipse of semi-major and semi-minor axes of 58 μm and 51 μm, respectively

et al. (2014) have demonstrated that the thickness of the SV, δ, is roughly constant for fixed experimental and processing parameters. In Fig. 4, the fit was for $\delta = 18.0\ \mu$m, and in Fig. 7, the fit was for $\delta = 15.5\ \mu$m. If one has already determined δ for the experiment, then it may be possible to determine which shape is more likely.

5. CONCLUSION

Because of the inherent optical limitations of performing Particle Image Velocimetry at the micron scale and the consequent data processing requirements, one must inevitably address the finite size of the region over which tracer particles are imaged. Rather than attempt to eliminate the effects of the finite size, we have introduced the Sampling Volume as the effective region over which particles are imaged and then contribute to the algorithms used to calculate the measured velocity fields. The result is often a quantitative determination of measured velocity profiles as well as inferred velocity fields throughout entire microchannels. Furthermore, one can use the SV concept to infer as much as possible about unknown experimental quantities, such as flow rates or channel shapes, greatly enhancing the practical utility of μPIV as a research and development tool.

6. ACKNOWLEDGMENTS

For the SEM images, we thank Michael Engel from IBM Research – Watson, as well as the LABNANO–CBPF. For help with calibration, we thank Diney Ether and the LPO–UFRJ. We would also like to thank José Florián at PUC–Rio for help with the μPIV equipment.

7. REFERENCES

Bryant, P.W., Neumann, R.F., Moura, M.J.B., Steiner, M., Carvalho, M.S. and Feger, C., 2014. "Quantitative μPIV for the measurement of velocity profiles". *arXiv:1407.5034*. URL `http://arxiv.org/abs/1407.5034`.

Chen, S. and Doolen, G.D., 1998. "Lattice boltzmann method for fluid flows". *Annu. Rev. Fluid Mech.*, Vol. 30, No. 1, pp. 329–364.

Cierpka, C. and Kähler, C., 2012. "Particle imaging techniques for volumetric three-component (3d3c) velocity measurements in microfluidics". *J. Vis.*, Vol. 15, No. 1, pp. 1–31.

Joseph, P. and Tabeling, P., 2005. "Direct measurement of the apparent slip length". *Phys. Rev. E*, Vol. 71, No. 3, p. 035303.

Kloosterman, A., Poelma, C. and Westerweel, J., 2011. "Flow rate estimation in large depth-of-field micro-PIV". *Exp. Fluids*, Vol. 50, No. 6, pp. 1587–1599.

Lindken, R., Rossi, M., Große, S. and Westerweel, J., 2009. "Micro-particle image velocimetry (μPIV): Recent developments, applications, and guidelines". *Lab Chip*, Vol. 9, No. 17, pp. 2551–2567.

Meinhart, C.D., Wereley, S.T. and Santiago, J.G., 1999. "PIV measurements of a microchannel flow". *Exp. Fluids*, Vol. 27, No. 5, pp. 414–419.

Olsen, M. and Adrian, R., 2000. "Out-of-focus effects on particle image visibility and correlation in microscopic particle image velocimetry". *Exp. in Fluids*, Vol. 29, No. 1, pp. S166–S174.

Rossi, M., Segura, R., Cierpka, C. and Kähler, C.J., 2012. "On the effect of particle image intensity and image preprocessing on the depth of correlation in micro-piv". *Exp. Fluids*, Vol. 52, No. 4, pp. 1063–1075.

Sott, K., Gebäck, T., Pihl, M., Lorén, N., Hermansson, A.M., Heintz, A. and Rasmuson, A., 2013. "μpiv methodology using model systems for flow studies in heterogeneous biopolymer gel microstructures". *Journal of colloid and interface science*, Vol. 398, pp. 262–269.

Tsai, P., Peters, A.M., Pirat, C., Wessling, M., Lammertink, R.G. and Lohse, D., 2009. "Quantifying effective slip length over micropatterned hydrophobic surfaces". *Phys. Fluids*, Vol. 21, No. 11, p. 112002.

Westerweel, J., Geelhoed, P. and Lindken, R., 2004. "Single-pixel resolution ensemble correlation for micro-PIV applications". *Exp. Fluids*, Vol. 37, No. 3, pp. 375–384.

Williams, S.J., Park, C. and Wereley, S.T., 2010. "Advances and applications on microfluidic velocimetry techniques". *Microfluid Nanofluid*, Vol. 8, No. 6, pp. 709–726.

8. RESPONSIBILITY NOTICE

The authors are the only responsible for the printed material included in this paper.